AGU PUBLICATIONS

JGR

Journal of Geophysical Research: Atmospheres

RESEARCH ARTICLE
10.1002/2013JD021388

Key Points:
- Largest database of glyoxal in the MBL
- Levels of glyoxal in the MBL are lower than previously reported
- Additional source of glyoxal needed to explain observations

Correspondence to:
A. Saiz-Lopez,
a.saiz@csic.es

Citation:
Mahajan, A. S., et al. (2014), Glyoxal observations in the global marine boundary layer, *J. Geophys. Res. Atmos.*, *119*, 6160–6169, doi:10.1002/2013JD021388.

Received 18 DEC 2013
Accepted 8 APR 2014
Accepted article online 13 APR 2014
Published online 16 MAY 2014

Glyoxal observations in the global marine boundary layer

Anoop S. Mahajan[1,2], Cristina Prados-Roman[1], Timothy D. Hay[1,3], Johannes Lampel[4], Denis Pöhler[4], Katja Großmann[4], Jens Tschritter[4], Udo Frieß[4], Ulrich Platt[4], Paul Johnston[3], Karin Kreher[3,5], Folkard Wittrock[6], John P. Burrows[6], John M.C. Plane[7], and Alfonso Saiz-Lopez[1]

[1]Atmospheric Chemistry and Climate Group, Institute of Physical Chemistry Rocasolano, CSIC, Madrid, Spain, [2]Indian Institute of Tropical Meteorology, Pune, India, [3]National Institute of Water and Atmospheric Research, Lauder, New Zealand, [4]Institute of Environmental Physics, University of Heidelberg, Heidelberg, Germany, [5]Bodeker Scientific, Alexandra, New Zealand, [6]Institute of Environmental Physics, University of Bremen, Bremen, Germany, [7]School of Chemistry, University of Leeds, Leeds, UK

Abstract Glyoxal is an important intermediate species formed by the oxidation of common biogenic and anthropogenic volatile organic compounds such as isoprene, toluene, and acetylene. Although glyoxal has been shown to play an important role in urban and forested environments, its role in the open ocean environment is still not well understood, with only a few observations showing evidence for its presence in the open ocean marine boundary layer (MBL). In this study, we report observations of glyoxal from 10 field campaigns in different parts of the world's oceans. These observations together represent the largest database of glyoxal in the MBL. The measurements are made with similar instruments that have been used in the past, although the open ocean values reported here, average of about 25 parts per trillion by volume (pptv) with an upper limit of 40 pptv, are much lower than previously reported observations that were consistently higher than 40 pptv and had an upper limit of 140 pptv, highlighting the uncertainties in the differential optical absorption spectroscopy method for the retrieval of glyoxal. Despite retrieval uncertainties, the results reported in this work support previous suggestions that the currently known sources of glyoxal are insufficient to explain the average MBL concentrations. This suggests that there is an additional missing source, more than a magnitude larger than currently known sources, which is necessary to account for the observed atmospheric levels of glyoxal. Therefore, it could play a more important role in the MBL than previously considered.

1. Introduction

Glyoxal (CHOCHO) is the smallest α-dicarbonyl compound in the atmosphere and is formed as an oxidation product of a number of volatile organic compounds (VOCs) like isoprene and monoterpenes. Initial interest in glyoxal within the atmospheric boundary layer was generated by reports of elevated concentrations at urban locations [*Grosjean et al.*, 1990; *Volkamer et al.*, 2005a; *Sinreich et al.*, 2007] and in forest environments [*Huisman et al.*, 2011; *MacDonald et al.*, 2012], with peak levels ranging between a few hundred parts per trillion (pptv, equivalent to pmol mol^{-1}) to low parts per billion (ppbv, equivalent to nmol mol^{-1}) observed using ground-based instruments. Satellite observations have also been reported using the Scanning Imaging Absorption Spectrometer for Atmospheric Cartography [*Wittrock*, 2006; *Wittrock et al.*, 2006], the Ozone Monitoring Instrument (K. Chance, personal communication, 2013), and the Global Ozone Monitoring Experiment-2 [*Lerot et al.*, 2010; *Vrekoussis et al.*, 2010]. These observations also see large values over forested regions and over locations with anthropogenic activities, in line with ground observations.

The known sources of glyoxal are biogenic (e.g., isoprene and monoterpenes) [*Spaulding et al.*, 2003; *Fu et al.*, 2008; *Stavrakou et al.*, 2009] and anthropogenic (such as aromatic compounds from vehicle emissions and biomass and fossil fuel burning) [*Volkamer et al.*, 2001, 2005a; *Fu et al.*, 2008]. Although large peak concentrations could be observed in urban areas mainly due to anthropogenic activity [*Volkamer et al.*, 2005a; *Sinreich et al.*, 2007], the largest global source of glyoxal is estimated to be the oxidation of biogenic VOC emissions, primarily isoprene [*Fu et al.*, 2008; *Stavrakou et al.*, 2009]. The total continental source of glyoxal to the atmosphere is constrained by satellite measurements to range between 94 and 108 Tg/yr, of which only about 50% is currently explained by known sources [*Fu et al.*, 2008; *Myriokefalitakis et al.*, 2008].

The atmospheric lifetime of glyoxal is of the order of 1–2 h for overhead sun conditions in urban environments [*Volkamer et al.*, 2005a, 2007], or 2–3 h globally [*Fu et al.*, 2008; *Myriokefalitakis et al.*, 2008], and

is determined by three main sink pathways—photolysis, reaction with OH, and loss due to uptake on aerosols [*Volkamer et al*., 2007]. The importance of glyoxal in secondary organic aerosol (SOA) formation has been an area of increased interest recently, although questions remain over the mechanism of glyoxal uptake[*Kroll et al*., 2005; *Liggio et al*., 2005; *Ervens and Volkamer*, 2010; *Nakao et al*., 2012]. Glyoxal uptake may also contribute to the missing source of SOA in the free troposphere identified in current global models such as GEOS-Chem [*Heald*, 2005; *Tan et al*., 2009].

Although several observations of glyoxal have been reported in the past (see above), most observations were performed over land and questions remain about its distribution over the remote ocean. Satellite-based measurements have indicated the presence of significant levels of glyoxal over the tropical oceans [*Wittrock et al*., 2006; *Lerot et al*., 2010; *Vrekoussis et al*., 2010]. These observations show vertical columns exceeding 5×10^{14} molecules cm^{-2}, which is equivalent to a concentration of at least 200 pptv if the glyoxal is confined within a boundary layer of 1000 m. These observations, in combination with model assumptions, indicate that tropical oceans could add up to 20 Tg/yr to the global glyoxal source [*Myriokefalitakis et al*., 2008]. However, the retrieved glyoxal abundances from different satellite observations are not consistent with retrieval issues related to low albedo over oceans, cloud coverage, and interference from water absorption and ring spectra. Furthermore, global glyoxal distributions using atmospheric models show a mismatch with satellite measurements in remote tropical ocean regions, where the models predict very low levels of glyoxal [*Fu et al*., 2008; *Myriokefalitakis et al*., 2008; *Stavrakou et al*., 2009].

This discrepancy highlights the need for ground-based observations to validate the satellite observations. A recent study was conducted in the eastern Pacific Ocean, where glyoxal observations of up to 140 pptv were reported [*Sinreich et al*., 2010] using the multi-axis differential optical absorption spectroscopy (MAX-DOAS) method. The authors suggested that the VOC concentrations needed to explain that about 100 pptv of glyoxal are either 600 pptv of isoprene, 2.8 ppbv toluene, or 8.9 ppbv acetylene, or lower concentrations if multiple compounds were present. However, the currently measured isoprene concentrations do not exceed 40 pptv in the marine boundary layer (MBL) and are mostly in the order of 10 pptv [*Sinreich et al*., 2010]. Thus, these reported observations, which show some agreement with satellite data, cannot be fully explained using the current knowledge of glyoxal source and sink chemistry, and considerable work is currently being done to discover a new source for glyoxal in the remote ocean environment.

Here we report observations of glyoxal using the MAX-DOAS and the long-path DOAS (LP-DOAS) methods in the MBL in different parts of the oceans over multiple years. This large database is then used to estimate the distribution of glyoxal and check whether an extra source is necessary to explain the observations or whether our understanding of the current sources and sinks is sufficient to explain them.

2. Experiment

Observations of glyoxal were made using the MAX-DOAS and LP-DOAS method during 10 field campaigns. Seven of those campaigns took place on scientific cruises in the Atlantic (*Polarstern* ANT-26 (October 2009 to January 2010) and ANT-28 (October 2010 to January 2011)), Pacific (HaloCAST-P (March–April 2010), TransBrom (October 2009), and SHIVA (November 2011)), and Indian and Southern Oceans (MALASPINA (December 2010 to July 2011) and SOAP (February 2012 to April 2013)); while three land-based studies were made at the Cape Verde Islands in the eastern Atlantic Ocean (HALOCAVE (June–November 2010)); Galapagos Islands, Ecuador, in the eastern Pacific Ocean (CHARLEX (September 2010 to March 2011)); and Shag Point, New Zealand, in the southern Pacific Ocean (HALMA (February–April 2013)). The LP-DOAS method was used during the HALOCAVE campaign at Cape Verde and CHARLEX campaign at the Galapagos Islands, while MAX-DOAS was used in every other campaign, including the CHARLEX campaign. A map with all the locations and cruise tracks is shown in Figure 1, along with the names of the campaigns during which the measurements were made.

Both, MAX-DOAS and LP-DOAS make use of the well-established differential optical absorption spectroscopy (DOAS) method, which has been used on several different platforms including ground, balloon, aircraft, and satellites [*Perner and Platt*, 1979; *Plane and Saiz-lopez*, 2006; *Platt and Stutz*, 2008]. DOAS allows the detection of weak absorption features and thus has high sensitivity that can be used to detect molecules such as glyoxal, which have low concentrations in the atmosphere. The MAX-DOAS method uses scattered sunlight from different viewing elevation angles, which provides a cost-effective and robust method for measurement

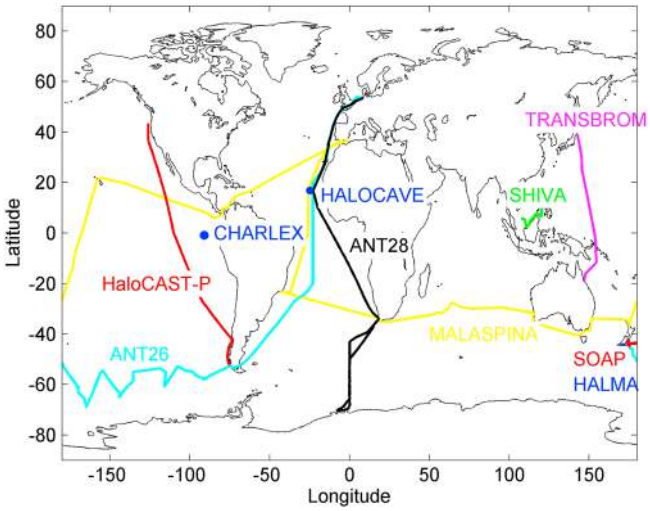

Figure 1. Map showing the locations and cruise tracks of the 10 field campaigns presented in this study. The campaign names are written beside the locations.

of trace gas differential slant column densities (DSCDs) in different environments [*Hönninger et al*., 2004; *Wagner*, 2004; *Wittrock et al*., 2004]. The DSCDs can then be converted into mixing ratios by the use of air mass factors, which can be calculated using radiative transfer modeling or the O_4 slant columns for the lower layers [*Platt and Stutz*, 2008]. The LP-DOAS method uses a Xe lamp as a light source, with a Newtonian telescope housing or fiber LP-DOAS telescope acting as both the transmitting and receiving optics. The advantage of this method is the fact that the atmospheric light path is known, and hence the derivation of mixing ratios is direct. The LP-DOAS instrument involved in the CHARLEX study has been used in several studies before, and details can be found elsewhere [*Plane and Saiz-lopez*, 2006; *Mahajan et al*., 2011; *Gómez Martín et al*., 2013], while the instrument used in HALOCAVE has also been used several times in the past, and details of the instrumental setup at Cape Verde have been given elsewhere [*Carpenter et al*., 2011].

In the case of the glyoxal retrieval using DOAS, several different analysis procedures have been commonly used [*Sinreich et al*., 2010; *Li et al*., 2012; *Liu et al*., 2012; *MacDonald et al*., 2012]. Most of the retrievals involve two major CHOCHO absorption bands including one at about 440 nm and the relatively strong band at around 455 nm. The differences in the analysis procedures are mainly due to the treatment of the large water vapor absorption structures in the same spectral window. The first and most common method of analysis is the traditional DOAS analysis, during which all the contributions of individual species to the differential optical density spectra are determined by simultaneously fitting their laboratory-measured absorption cross sections using singular value decomposition. For MAX-DOAS glyoxal measurements, either the 420–460 nm window or the 433–460 nm spectral window are normally used including glyoxal [*Volkamer et al*., 2005b], water vapor [*Rothman et al*., 2013], iodine oxide [*Spietz et al*., 2005], oxygen dimer [*Hermans*, 2002], nitrogen dioxide [*Vandaele et al*., 1997], ozone [*Bogumil et al*., 2003], and a ring spectrum [*Chance and Spurr*, 1997] as the absorbers, in addition to a third-order polynomial for generating the differential optical spectra and the zenith spectrum from each elevation angle scan sequence as the reference spectrum. An example of the spectral fits using this method is shown in Figure 2. The LP-DOAS data analysis uses similar spectral windows and absorbers except ozone and the ring spectrum. As reference spectrum, a measurement of the light source itself is used. The largest source of structure in the residual is due to the water vapor absorption, which peaks around 443 nm in the chosen window. To reduce the structure remaining in the residual, the second retrieval method uses a gap for the strong water vapor absorption features rather than the whole spectral window, ensuring that the glyoxal absorption bands are not affected. This gap generally leads to an improvement in the root-mean-square (RMS) of the residual and hence the detection limit in comparison to the first method, if based on the RMS. Our tests indicated that using the second method leads to lower DSCDs, by about 10–15% for most of the campaigns, but even lower (up to 70% lower for DSCDs $> 1 \times 10^{15}$ molecules cm^{-2} compared to using no gap during the TransBrom campaign) for others, although the improvement in the noise can be about a factor of 2 due to the gap over the large water absorption features. The third method of retrieval is using a water vapor cross section derived from the atmospheric measurements using a ratio of spectra at different elevation angles [*Sinreich et al*., 2010]. This method leads to the best signal-to-noise ratio because the water vapor reference spectrum is derived by the instrument itself; its specific optical properties inherently lead to better spectral retrieval with less systematic structures. For this procedure to succeed, it is necessary to have measurement spectra without any glyoxal absorption, but a strong water vapor absorption signal, to avoid interferences from the beginning. If, as suggested by *Sinreich et al.* [2010], glyoxal is ubiquitous on the open

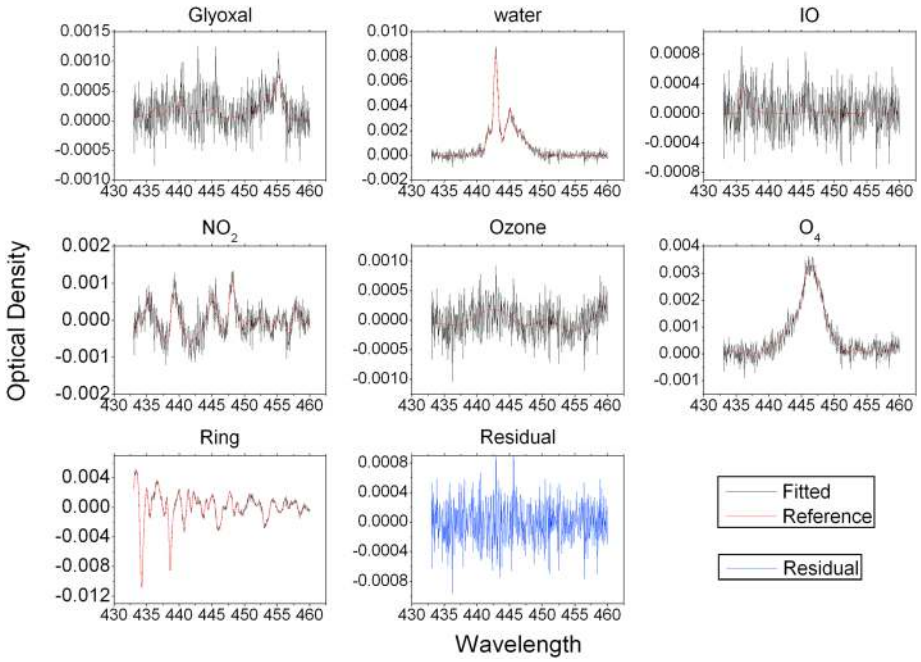

Figure 2. Example of DOAS spectral fits for glyoxal during the MALASPINA study at Solar Zenith Angle (SZA) = 23° on 23 July 2011 at 11:08 A.M. for an elevation angle of 2°. The column densities retrieved were glyoxal (1.2×10^{15} molecules cm^{-2}), H_2O (2.2×10^{23} molecules cm^{-2}), IO (1.4×10^{13} molecules cm^{-2}), NO_2 (4.6×10^{15} molecules cm^{-2}), O_3 (4.5×10^{18} molecules cm^{-2}), O_4 (6.4×10^{43} molecules^2 cm^{-5}), and RMS (3.9×10^{-4}).

ocean, this is difficult. Using this method, during the CHARLEX, HaloCAST-P, and MALASPINA campaigns, the retrieved DSCDs were different than the first two methods. The difference was not a constant offset, and we were not able to observe any strong dependence on measured parameters. An example of comparison of fits using the three major different methods is shown in Figure 3, in which the third method retrieves 30–40% larger DSCD than the earlier two methods. However, it should be noted that this increase is dependent on the spectrum, time, and location and is not a constant increase. We should however point out that similar tests in the past by some other groups showed that the glyoxal DSCDs were not affected by using this artificial cross section, although the detection limits were greatly improved [*Sinreich et al.*, 2010]. Unfortunately, no recommended glyoxal settings to use for DOAS analysis exist at the moment, and the DOAS community needs to address this through intercomparison campaigns in regions with low glyoxal levels, close to the detection limit of the instrument, and comparison to other measurement techniques, to ascertain the robustness of the analysis procedures used. For this study, we use either of the first two methods, i.e., using laboratory-measured absorption cross sections with or without a gap in the analysis spectral window. The retrievals are done either with the commonly used analysis programs QDOAS/WinDOAS [*Fayt and Van Roozendael*, 2013], DOASIS [*Lehmann*, 2013], NLIN_D [*Richter et al.*, 1999] or in the case of SOAP and HALMA, with code developed at National Institute of Water and Atmospheric Research (NIWA) (by Paul Johnston) [*Vandaele et al.*, 2005]. A summary of the retrieval settings used herein are given in Table 1. An opportunity to run an intercomparison study between two instruments at the same place was presented during the TransBrom study, where two MAX-DOAS instruments, belonging to the Institute of Environmental Physics, University of Heidelberg, Heidelberg, Germany (IUP-UH), and the Institute of Environmental Physics, University of Bremen, Bremen, Germany (IUP-UB), were present. The comparison between the two retrievals for the 3° elevation angle, for data above the detection limit of the instruments, is presented in Figure 4. The r^2 was 0.19, and the gradient of the linear fit between the two data was 0.25. The IUP-UH data, which were retrieved using a 420–460 nm window, with a gap for the water vapor from 441–447 nm, were consistently lower than the IUP-UB-retrieved DSCDs, which were retrieved using a window of 424–458 nm, without any gap and the differences increased at larger DSCDs. It should be noted that the comparison is difficult due to different sampling strategies; for example, the IUP-UB instrument had more elevation angles and changes in the azimuth direction, while the IUP-UH instrument did not.

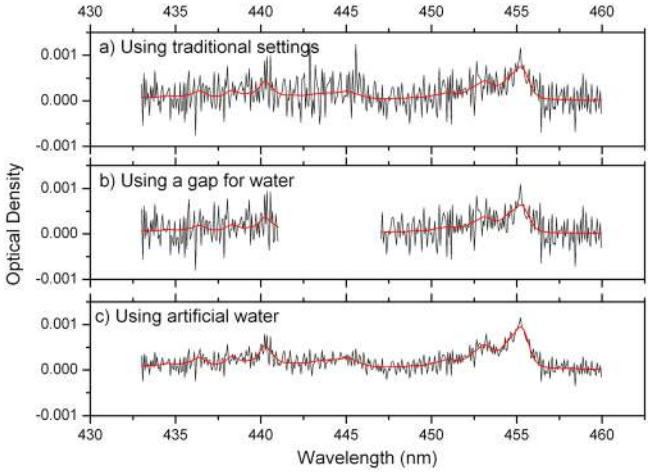

Figure 3. Differences in glyoxal DOAS analysis using the three methods described in the text. (a) Traditional DOAS method using laboratory-measured cross sections and no gap (CHOCHO DSCD = 1.3×10^{15} molecules cm^{-2}); (b) using laboratory-measured cross sections and a gap for water absorption features, which reduces the noise (CHOCHO DSCD = 1.2×10^{15} molecules cm^{-2}); and (c) using an artificial water vapor cross section created using spectra measured in the field, which greatly reduces the noise (CHOCHO DSCD = 1.7×10^{15} molecules cm^{-2}).

A series of filters were applied to the data to ensure the quality of the retrieved DSCDs used for further analysis and comparison. The data were filtered for solar zenith angles greater than 65°, an RMS of greater than 2.5×10^{-3}, and a cloud index. The cloud index (0 – clear sky, 1 – cloudy sky) is a metric for estimating the sky conditions. The filter is calculated using a ratio of radiation fluxes from the edges of the spectral window (420 nm and 459 nm) and elevation angles measured using the MAX-DOAS instrument in order to distinguish the predominant scattering conditions. This ratio was calculated between the zenith and the lowest elevation angles, with a low ratio indicating a cloudy environment. This ratio is used in conjunction with radiometer data, and the DOAS-retrieved O_4 DSCDs. A threshold of 1.1 was calculated, above which the conditions were cloud free (cloud index of 0). It is difficult to compute the uncertainties on the cloud index; in fact, the filter is a stringent cutoff. This would mean that the cloud filter procedure is conservative, with a risk of disregarding some valid data near the threshold, but it ensures that only data from clear sky conditions were used for further analysis. A similar filter has been used previously by other groups for similar studies [*Sinreich et al.*, 2010; *Mahajan et al.*, 2012].

3. Results and Discussion

Figure 5 shows the MAX-DOAS glyoxal DSCDs along different viewing angles for all the campaigns included in this study. It can be seen that for most of the studies, the DSCDs at 3° elevation angle (or 2° for MALASPINA, SOAP, and HALMA) are less than 2×10^{15} molecules cm^{-2}. In some cases, higher DSCDs were observed when the ships were closer to the coast; e.g., during SHIVA, DSCDs peaking at ~3×10^{15} molecules cm^{-2} were observed on the last day of the cruise close to Manila, while elevated DSCDs during the MALASPINA study were only observed close to the sea ports. Our measurements show that the glyoxal DSCDs in most of the remote MBL are an average of 2.5 times (ranging between 1.5 and 5 times) lower than past reports of elevated DSCDS, which were up to 3.5×10^{15} molecules cm^{-2} at 1.5° elevation angle or 2.5×10^{15} molecules cm^{-2} at 3.8° [*Sinreich et al.*, 2010]. A consistent feature across the different campaigns in the present study is that lower elevation angles display higher DSCDs, indicating enhanced glyoxal concentrations in the lower troposphere.

For selected days during the CHARLEX study, where at least three viewing elevation angles pass the quality and cloud filters, volume mixing ratios were retrieved from the MAX-DOAS DSCDs following the so-called O_4 method [*Wagner*, 2004] to estimate the scattering properties of the atmosphere and using the NIMO fully spherical Monte Carlo radiative transfer model [*Hay et al.*, 2012]. This procedure is explained in detail in a previous paper on ship-based MAX-DOAS measurements in the eastern Pacific [*Mahajan et al.*, 2012]. Briefly, an aerosol profile is estimated in order to reproduce the observed DSCDs of O_4, whose vertical distribution is well known and is proportional to the square of the O_2 concentration. Parameterized aerosol profiles with varying aerosol optical depths and shapes were prescribed, and the profile parameters are floated to obtain the best match between the forward modeled and the observed O_4 DSCDs. The surface glyoxal mixing ratios estimated using this method resulted in values less than 40 pptv in the open ocean environment.

Glyoxal was not observed above the detection limit of the LP-DOAS during the 8 month CHARLEX study on the Galapagos Islands in the eastern Pacific or the HALOCAVE study on the Cape Verde Islands. The range of mixing ratios retrieved from the MAX-DOAS-based DSCDs stayed below the detection limit of 50 pptv of the

Table 1. Summary of the 10 Field Campaigns as Well as the MAX and LP-DOAS Settings and Software Used for the Retrieval of Glyoxal Presented in This Work[a]

Campaign Name	Group	Location	Dates	Glyoxal Retrieval Settings	Software
			MAX-DOAS		
ANT-26 (R/V *Polarstern*)	UH	Atlantic Ocean, Southern Ocean	10/2009–01/2010	420–460 nm window, gap for water absorption	DOASIS
ANT-28 (R/V *Polarstern*)	UH	Atlantic Ocean, southern Pacific Ocean	10/2011–01/2012	420–460 nm window, gap for water absorption	DOASIS
HaloCAST-P	CSIC	Eastern Pacific Ocean	03/2010–04/2010	433–460 nm window, no gap	QDOAS
TransBrom (R/V *Sonne*)	UH and UB	Western Pacific Ocean	10/2009	420–460 nm window, gap for water absorption; 424–458 nm window	WinDOAS and IUP-UB NLIN_D code
SHIVA (R/V *Sonne*)	UB	Western Pacific Ocean	11/2011	424–458 nm window	IUP-UB NLIN_D code
MALASPINA	CSIC	Parts of the Atlantic Ocean, Pacific Ocean, Indian Ocean, and Southern Ocean	12/2010–07/2011	433–460 nm window, no gap	QDOAS
SOAP	NIWA	Southern Pacific Ocean	02/2012–04/2013	433–460 nm window, no gap	NIWA code
CHARLEX	CSIC	Galapagos Islands, Ecuador; eastern Pacific Ocean	09/2010–03/2011	433–460 nm window, no gap	QDOAS
HALMA	NIWA	Shag Point, New Zealand	02/2013–04/2013	433–460 nm window, no gap	NIWA code
			LP-DOAS		
HALOCAVE	UH	Cape Verde Islands, eastern Atlantic Ocean	06/2010–11/2010	433–460 nm window, no gap	DOASIS
CHARLEX	CSIC	Galapagos Islands, Ecuador; eastern Pacific Ocean	09/2010–03/2011	433–460 nm window, no gap	QDOAS and custom-built code

[a]Groups: CSIC - Institute of Physical Chemistry Rocasolano, CSIC, Madrid, Spain; NIWA - National Institute of Water and Atmospheric Research (NIWA), Lauder, New Zealand; IUP-UH - Institute of Environmental Physics, University of Heidelberg, Heidelberg, Germany; and IUP-UB - Institute of Environmental Physics, University of Bremen, Bremen, Germany.

LP-DOAS instrument during the CHARLEX study, corresponding to an RMS of ~5×10^{-4} and a path length of ~9 km. Similar results were obtained during the HALOCAVE study on the Cape Verde Islands, where glyoxal was not observed above the instrumental detection limit (7–19 June 2010, path length ~5.6 km, detection limit 48 pptv; 19–20 June 2010, path length ~12.6 km, detection limit 42 pptv; 20 June to 26 October 2010, path length ~12.6 km, detection limit 60 pptv; and 30 October to 11 November 2010, path length ~12.6 km, detection limit 60 pptv). The detection limits vary due to different absorption path lengths and xenon lamps. In the past, a long-term study (November 2006 to July 2007) on the Cape Verde Islands in the Atlantic Ocean also reported an absence of glyoxal above the LP-DOAS detection limit of about 150 pptv, two sigma [*Mahajan et al.*, 2011]. This range of mixing ratios is lower than past reports over the eastern Pacific, where estimates were up to 140 pptv [*Sinreich et al.*, 2010]. It should be noted that the past reports were done in different years, which could explain the differences in retrieved DSCDs. The data reported by *Sinreich et al.* [2010] were acquired in October–November 2008, which does not overlap with any of the periods reported here (see Figure 5). However, it is also likely that the differences are due to DOAS analysis methods, as explained in section 2, and hence further work is necessary to ascertain the best settings for stable glyoxal retrievals.

Figure 6 shows the geographical distribution of glyoxal as a day-averaged composite of the lowermost elevation angle of all the studies included here. The land-based studies where MAX-DOAS observations were available (CHARLEX and HALMA) have been time averaged for the entire measurement period. It can be seen that the glyoxal DSCDs are low over most of the world's oceans, with a

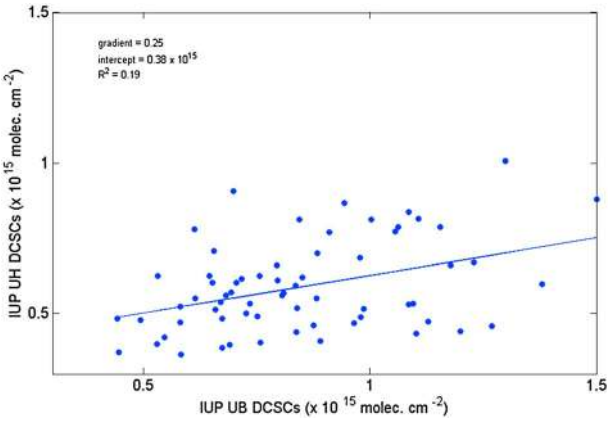

Figure 4. A comparison of the differential slant column densities above the detection limit for the 3° elevation angle during the TransBrom campaign in the western Pacific is shown. Two MAX-DOAS instruments (University of Heidelberg (UH) and University of Bremen (UB)) were involved in the study and showed a weak correlation and a large difference in the absolute DSCDs. It should be noted that the comparison is difficult due to different sampling strategies; for example, the IUP-UB instrument had more elevation angles and changes in the azimuth direction, while the IUP-UH instrument did not.

few high values close to the coast, and in East Asia compared to the rest of the campaigns. In most of the global MBL, the glyoxal columns are under the detection limit of the instruments, which depended on the study. Interestingly, there is a lack of a clear increase of glyoxal in the tropics, contrary to what has been suggested by satellite observations in the past [*Lerot et al.*, 2010; *Vrekoussis et al.*, 2010]. The satellite retrieval indicates that there should be an increase in the tropics, although the open ocean values are close to the detection limit ($2–3 \times 10^{14}$ molecules cm^{-2}). This increase, when compared to the northern midlatitudes, was not observed by the surface studies, even though during ANT-28 potentially the outflow from Africa was observed, as it can be observed from a satellite [*Vrekoussis et al.*, 2010]. Note that over the open ocean, satellite retrievals are difficult to perform due to the low albedo

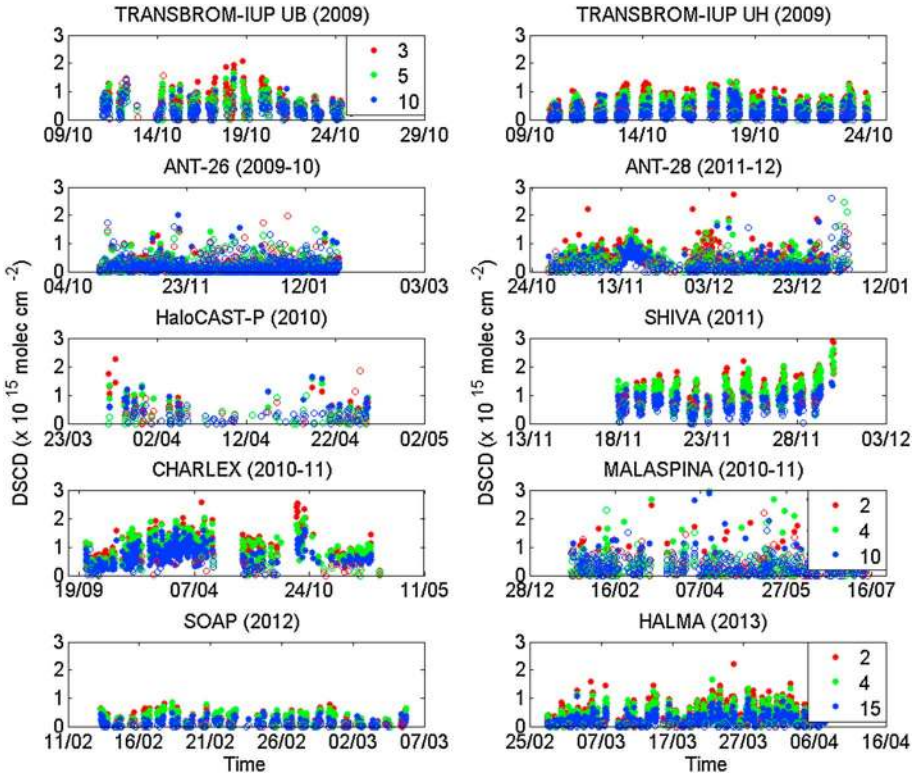

Figure 5. Differential slant column densities of glyoxal along different viewing elevation angles are shown for the 10 campaigns. During the TransBrom study, there were two MAX-DOAS on the same cruise (IUP-UB - Institute of Environmental Physics, Bremen, and IUP-UH - Institute of Environmental Physics, Heidelberg) with the same line of sight (for instrument description of IUP-UB and IUP-UH, see *Peters et al.* [2012] and of *Großmann et al.* [2013], respectively). Empty circles indicate data under the detection limit, whereas filled circles show data above the detection limit. Please note that during MALASPINA and HALMA, the lower viewing angles were different from the rest of the campaigns.

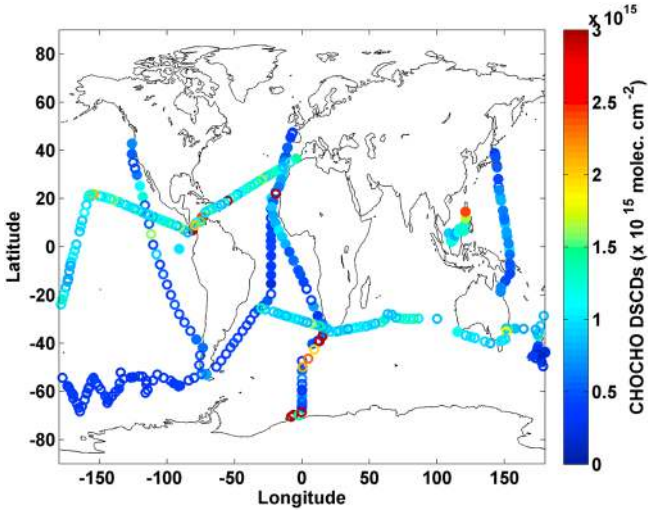

Figure 6. Daily averaged DSCDs of glyoxal for the lowest elevation angle from campaigns included in this study are shown. Empty circles indicate that the DSCDs were below the detection limit of the instruments, while filled circles indicate data above the detection limit. The long-term observations on islands have been averaged for the entire study period.

and interference from the water vapor spectra, absorption by liquid water [*Pope and Fry*, 1997; *Richter et al*., 2011], and vibrational Raman scattering in water [*Vountas et al*., 2003], and hence open ocean retrievals should be regarded carefully. This applies for ground measurements as well, since for the lowest elevation angles (<10°) of ground measurements, about 10–15% of the measured photons have been in contact with ocean surface water [*Großmann et al*., 2013]. It is also possible that the satellite observes an elevated layer of glyoxal, but this would have to be geographically restricted to a few regions, rather than widespread in the free troposphere. One of the main interferences in the wavelength window utilized for retrieval of glyoxal has been recognized to be the absorption by liquid water [*Richter et al*., 2011], and it is possible that this effect is still not completely accounted for considering the largest differences seen in the tropical region.

The satellite captures the elevated concentrations in East Asia similar to the SHIVA campaign [*Vrekoussis et al*., 2010]. Higher column densities are also observed over land, which is supported by previous land-based campaigns [*Volkamer et al*., 2005a; *MacDonald et al*., 2012], and the fact that elevated DSCDs were observed closer to the coast in most of the studies included here. Thus, there is a discrepancy between the satellite observations and the ground-based studies, which needs to be explored further in addition to the uncertainties in the DOAS analysis procedure.

The most important natural precursors of glyoxal are known to be isoprene (8% yield [*Bey et al*., 2001]), and acetylene (65% yield [*Hatakeyama et al*., 1986]). Assuming an OH concentration of 0.12 pptv and an atmospheric lifetime for CHOCHO of 2 h, the VOC concentration needed to explain 25 pptv of glyoxal (average from all studies) is 150 pptv of isoprene or 2.5 ppbv acetylene, or lower concentrations if multiple VOC sources of glyoxal are present. Isoprene concentrations in the MBL are much lower than 150 pptv, typically around 10 pptv [*Palmer*, 2005], while concentrations of acetylene are in the range of 200 pptv [*Carpenter et al*., 2011]. Thus, based on the data presented herein, it is likely that an additional source of glyoxal is still necessary to explain the MBL background mixing ratios, even if they are lower than previously reported [*Sinreich et al*., 2010]. There is growing evidence for a seawater source of glyoxal [*Pinxteren and Herrmann*, 2013], although there is still no clear picture on the exact nature of the source or its strength.

4. Conclusions

MAX-DOAS and LP-DOAS observations of glyoxal were made in different parts of the world's oceans during 10 field campaigns between 2009 and 2013. The observations indicate that the levels of glyoxal in the MBL are lower than previously estimated. They are, however, still larger than what the known sources of glyoxal can account for. There is also a discrepancy between the satellite estimations and the data presented here, indicating shortcomings in the retrieval procedures of glyoxal. We encourage the DOAS community to conduct thorough testing of the DOAS retrieval of glyoxal, especially in areas with low levels close to instrumental detection limits. Further studies are required to rule out the influence of water cross sensitivities on glyoxal retrievals. Moreover, the results presented here highlight the need of additional investigations on a possible new source of glyoxal in order to explain the concentrations measured in the remote open ocean environment.

Acknowledgments

The data supporting this article can be requested from the corresponding author (a.saiz@csic.es). We thank the logistical support from the MALASPINA 2010 project funded by the Spanish Ministry of Science and Innovation and S.-J. Royer for instrumental support during MALASPINA. Indian Institute of Tropical Meteorology is supported by the Ministry of Earth Sciences, Government of India. We thank J.-C. Gómez Martín, for useful discussions and helping with the CHARLEX, HaloCAST-P, and MALASPINA field campaigns. For the HALOCAVE project, we would like to acknowledge L.J. Carpenter, L.M. Mendes, University of Leeds, and the German Federal Ministry of Education and Research for funding. The national WGL project TransBrom aboard the R/V *Sonne* was supported by the BMBF (German Federal Ministry of Education and Research) through grant 03G0731A and the project EU-SHIVA through grant FP7-ENV-2007-1-226224. Additional funding from the projects SOPRAN (03F0462F) (funded by BMBF, the German Federal Ministry of Education and Research), MAORI (DFG-PO 1801/1-1), and HALMA (BMBF 01DR12100) is acknowledged.

References

Bey, I., D. J. Jacob, R. M. Yantosca, J. A. Logan, B. Field, A. M. Fiore, Q. B. Li, H. Liu, J. L. Mickley, and M. G. Schultz (2001), Global modeling of tropospheric chemistry with assimilated meteorology: Model description and evaluation, *J. Geophys. Res.*, *106*, 23,073–23,096, doi:10.1029/2001JD000807.

Bogumil, K., et al. (2003), Measurements of molecular absorption spectra with the SCIAMACHY pre-flight model: Instrument characterization and reference data for atmospheric remote-sensing in the 230–2380 nm region, *J. Photochem. Photobiol. A Chem.*, *157*(2–3), 167–184, doi:10.1016/S1010-6030(03)00062-5. [Available at http://linkinghub.elsevier.com/retrieve/pii/S1010603003000625.]

Carpenter, L. J., et al. (2011), Seasonal characteristics of tropical marine boundary layer air measured at the Cape Verde Atmospheric Observatory, *J. Atmos. Chem.*, *67*(2–3), 87–140, doi:10.1007/s10874-011-9206-1. [Available at http://link.springer.com/10.1007/s10874-011-9206-1, Accessed 9 January 2012.]

Chance, K. V., and R. J. Spurr (1997), Ring effect studies: Rayleigh scattering, including molecular parameters for rotational Raman scattering, and the Fraunhofer spectrum., *Appl. Opt.*, *36*(21), 5224–5230. [Available at http://www.ncbi.nlm.nih.gov/pubmed/18259337.]

Ervens, B., and R. Volkamer (2010), Glyoxal processing by aerosol multiphase chemistry: Towards a kinetic modeling framework of secondary organic aerosol formation in aqueous particles, *Atmos. Chem. Phys.*, *10*(17), 8219–8244, doi:10.5194/acp-10-8219-2010. [Available at http://www.atmos-chem-phys.net/10/8219/2010/, Accessed 6 June 2013.]

Fayt, C., and M. Van Roozendael (2013), QDOAS 1.00. Software User Manual. [Available at http://uv-vis.aeronomie.be/software/QDOAS/.]

Fu, T. M., D. J. Jacob, F. Wittrock, J. P. Burrows, M. Vrekoussis, and D. K. Henze (2008), Global budgets of atmospheric glyoxal and methylglyoxal, and implications for formation of secondary organic aerosols, *J. Geophys. Res.*, *113*, D15303, doi:10.1029/2007JD009505.

Gómez Martín, J. C., et al. (2013), Iodine chemistry in the eastern Pacific marine boundary layer, *J. Geophys. Res. Atmos.*, *118*, 1–18, doi:10.1002/jgrd.50132.

Grosjean, D., A. H. Miguel, and T. M. Tavares (1990), Urban air pollution in Brazil: Acetaldehyde and other carbonyls, *Atmos. Environ. Part B-Urban Atmos.*, *24*(1), 101–106.

Großmann, K., et al. (2013), Iodine monoxide in the Western Pacific marine boundary layer, *Atmos. Chem. Phys.*, *13*(6), 3363–3378, doi:10.5194/acp-13-3363-2013. [Available at http://www.atmos-chem-phys.net/13/3363/2013/, Accessed 24 October 2012.]

Hatakeyama, S., N. Washida, and H. Akimoto (1986), Rate constants and mechanisms for the reaction of OH (OD) radicals with acetylene, propyne, and 2-butyne in air at 297 +/- 2 K, *J. Phys. Chem.*, *90*, 173–178.

Hay, T. D., G. E. Bodeker, K. Kreher, R. Schofield, J. B. Liley, M. Scherer, and A. J. McDonald (2012), The NIMO Monte Carlo model for box-air-mass factor and radiance calculations, *J. Quant. Spectrosc. Radiat. Transfer*, *113*(9), 721–738, doi:10.1016/j.jqsrt.2012.02.005. [Available at http://linkinghub.elsevier.com/retrieve/pii/S0022407312000568, Accessed 20 March 2012.]

Heald, C. L. (2005), A large organic aerosol source in the free troposphere missing from current models, *Geophys. Res. Lett.*, *32*, L18809, doi:10.1029/2005GL023831.

Hermans, C. (2002), Measurement of absorption cross sections and spectroscopic molecular parameters: O_2 and its collisonal induced absorption. [Available at http://spectrolab.aeronomie.be/o2.htm.]

Hönninger, G., C. von Friedeburg, and U. Platt (2004), Multi axis differential optical absorption spectroscopy, *Atmos. Chem. Phys.*, *4*, 231–254, doi:10.5194/acp-4-231-2004.

Huisman, A. J., et al. (2011), Photochemical modeling of glyoxal at a rural site: Observations and analysis from BEARPEX 2007, *Atmos. Chem. Phys.*, *11*(17), 8883–8897, doi:10.5194/acpd-11-13655-2011. [Available at http://www.atmos-chem-phys-discuss.net/11/13655/2011/, Accessed 9 May 2011.]

Kroll, J. H., N. L. Ng, S. M. Murphy, V. Varutbangkul, R. C. Flagan, and J. H. Seinfeld (2005), Chamber studies of secondary organic aerosol growth by reactive uptake of simple carbonyl compounds, *J. Geophys. Res.*, *110*, D23207, doi:10.1029/2005JD006004.

Lehmann, T. (2013), DOASIS. [Available at https://doasis.iup.uni-heidelberg.de/bugtracker/projects/doasis/documentations.php.]

Lerot, C., T. Stavrakou, I. De Smedt, J.-F. Müller, and M. Van Roozendael (2010), Glyoxal vertical columns from GOME-2 backscattered light measurements and comparisons with a global model, *Atmos. Chem. Phys. Discuss.*, *10*(9), 21,147–21,188. [Available at http://www.atmos-chem-phys-discuss.net/10/21147/2010/.]

Li, X., T. Brauers, A. Hofzumahaus, K. Lu, Y. P. Li, M. Shao, T. Wagner, and A. Wahner (2012), MAX-DOAS measurements of NO_2, HCHO and CHOCHO at a rural site in Southern China, *Atmos. Chem. Phys. Discuss.*, *12*(2), 3983–4029, doi:10.5194/acpd-12-3983-2012. [Available at http://www.atmos-chem-phys-discuss.net/12/3983/2012/, Accessed 7 March 2012.]

Liggio, J., S.-M. Li, and R. McLaren (2005), Reactive uptake of glyoxal by particulate matter, *J. Geophys. Res.*, *110*, D10304, doi:10.1029/2004JD005113.

Liu, Z., et al. (2012), Exploring the missing source of glyoxal (CHOCHO) over China, *Geophys. Res. Lett.*, *39*, L10812, doi:10.1029/2012GL051645.

MacDonald, S. M., H. Oetjen, A. S. Mahajan, L. K. Whalley, P. M. Edwards, D. E. Heard, C. E. Jones, and J. M. C. Plane (2012), DOAS measurements of formaldehyde and glyoxal above a south-east Asian tropical rainforest, *Atmos. Chem. Phys.*, *12*(13), 5949–5962, doi:10.5194/acp-12-5949-2012. [Available at http://www.atmos-chem-phys-discuss.net/12/5903/2012/, Accessed 14 March 2012.]

Mahajan, A. S., L. K. Whalley, E. A. Kozlova, H. Oetjen, L. M. Mendes, K. L. Furneaux, A. Goddard, D. E. Heard, J. M. C. Plane, and A. Saiz-Lopez (2011), DOAS observations of formaldehyde and its impact on the HO_x balance in the tropical Atlantic marine boundary layer, *J. Atmos. Chem.*, *66*(3), 167–178, doi:10.1007/s10874-011-9200-7. [Available at http://www.springerlink.com/index/10.1007/s10874-011-9200-7, Accessed 29 August 2011.]

Mahajan, A. S., et al. (2012), Latitudinal distribution of reactive iodine in the Eastern Pacific and its link to open ocean sources, *Atmos. Chem. Phys.*, *12*, 11,609–11,617, doi:10.5194/acp-12-11609-2012.

Myriokefalitakis, S., M. Vrekoussis, K. Tsigaridis, F. Wittrock, A. Richter, C. Brühl, R. A. Volkamer, J. P. Burrows, and M. Kanakidou (2008), The influence of natural and anthropogenic secondary sources on the glyoxal global distribution, *Atmos. Chem. Phys.*, *8*(16), 4965–4981. [Available at http://www.atmos-chem-phys.net/8/4965/2008/.]

Nakao, S., Y. Liu, P. Tang, C.-L. Chen, J. Zhang, and D. R. Cocker III (2012), Chamber studies of SOA formation from aromatic hydrocarbons: Observation of limited glyoxal uptake, *Atmos. Chem. Phys.*, *12*, 3927–3937, doi:10.5194/acp-12-3927-2012. [Available at http://www.atmos-chem-phys.net/12/3927/2012/, Accessed 3 May 2012.]

Palmer, P. I. (2005), Quantifying global marine isoprene fluxes using MODIS chlorophyll observations, *Geophys. Res. Lett.*, *32*, L09805, doi:10.1029/2005GL022592.

Perner, D., and U. Platt (1979), Detection of nitrous acid in the atmosphere by differential optical absorption, *Geophys. Res. Lett.*, *6*, 917–920, doi:10.1029/GL006i012p00917.

Peters, E., F. Wittrock, K. Großmann, U. Frieß, A. Richter, and J. P. Burrows (2012), Formaldehyde and nitrogen dioxide over the remote western Pacific Ocean: SCIAMACHY and GOME-2 validation using ship-based MAX-DOAS observations, *Atmos. Chem. Phys.*, *12*(22), 11,179–11,197, doi:10.5194/acp-12-11179-2012. [Available at http://www.atmos-chem-phys.net/12/11179/2012/, Accessed 29 November 2012.]

Pinxteren, M. V., and H. Herrmann (2013), Glyoxal and methylglyoxal in Atlantic seawater and marine aerosol particles: Method development and first application during the Polarstern cruise ANT XXVII/4, *Atmos. Chem. Phys. Discuss.*, *13*, 15,301–15,331, doi:10.5194/acpd-13-15301-2013.

Plane, J. M. C., and A. Saiz-lopez (2006), UV-visible differential optical absorption spectroscopy (DOAS), in *Analytical Techniques for Atmospheric Measurement*, edited by D. E. Heard, pp. 147–188, Wiley-Blackwell, Oxford, U. K.

Platt, U., and J. Stutz (2008), *Differential Optical Absorption Spectroscopy: Principles and Applications First*, Springer, Berlin Heidelberg.

Pope, R. M., and E. S. Fry (1997), Absorption spectrum (380–700 nm) ofpure water. II. Integrating cavity measurements, *Appl. Opt.*, *36*(33), 8710–8723.

Richter, A., M. Eisinger, A. Ladstatter-Weissenmayer, and J. P. Burrows (1999), DOAS Zenith sky observations: 2. Seasonal variation of BrO over Bremen (53 degrees N) 1994–1995, *J. Atmos. Chem.*, *32*, 83–99.

Richter, A., M. Begoin, A. Hilboll, and J. P. Burrows (2011), An improved NO_2 retrieval for the GOME-2 satellite instrument, *Atmos. Meas. Tech.*, *4*(6), 1147–1159, doi:10.5194/amt-4-1147-2011. [Available at http://www.atmos-meas-tech.net/4/1147/2011/, Accessed 13 December 2013.]

Rothman, L. S., et al. (2013), The HITRAN 2012 molecular spectroscopic database, *J. Quant. Spectrosc. Radiat. Transfer*, *130*, 4–50, doi:10.1016/j.jqsrt.2013.07.002. [Available at http://linkinghub.elsevier.com/retrieve/pii/S0022407313002859, Accessed 13 November 2013.]

Sinreich, R., R. Volkamer, F. Filsinger, U. Frieß, C. Kern, U. Platt, O. Sebastian, and T. Wagner (2007), MAX-DOAS detection of glyoxal during ICARTT 2004, *Atmos. Chem. Phys.*, *7*, 1293–1303.

Sinreich, R., S. Coburn, B. Dix, and R. Volkamer (2010), Ship-based detection of glyoxal over the remote tropical Pacific Ocean, *Atmos. Chem. Phys.*, *10*(23), 11,359–11,371, doi:10.5194/acp-10-11359-2010. [Available at http://www.atmos-chem-phys.net/10/11359/2010/, Accessed 23 December 2010.]

Spaulding, R. S., G. Schade, A. H. Goldstein, and M. J. Charles (2003), Characterization of secondary atmospheric photooxidation products: Evidence for biogenic and anthropogenic sources, *J. Geophys. Res.*, *108*(D8), 4247, doi:10.1029/2002JD002478.

Spietz, P., J. C. Gómez Martín, and J. P. Burrows (2005), Spectroscopic studies of the I-2/O-3 photochemistry—Part 2. Improved spectra of iodine oxides and analysis of the IO absorption spectrum, *J. Photochem. Photobiol. A Chem.*, *176*(1–3), 50–67.

Stavrakou, T., J.-F. Müller, I. De Smedt, M. Van Roozendael, M. Kanakidou, M. Vrekoussis, F. Wittrock, A. Richter, and J. P. Burrows (2009), The continental source of glyoxal estimated by the synergistic use of spaceborne measurements and inverse modelling, *Atmos. Chem. Phys.*, *9*(21), 8431–8446, doi:10.5194/acp-9-8431-2009. [Available at http://www.atmos-chem-phys.net/9/8431/2009/.]

Tan, Y., M. J. Perri, S. P. Seitzinger, and B. J. Turpin (2009), Effects of precursor concentration and acidic sulfate in aqueous glyoxal-OH radical oxidation and implications for secondary organic aerosol, *Environ. Sci. Technol.*, *43*(21), 8105–8112, doi:10.1021/es901742f. [Available at http://www.pubmedcentral.nih.gov/articlerender.fcgi?artid=2771719&tool=pmcentrez&rendertype=abstract.]

Vandaele, A. C., C. Hermans, P. Simon, M. R. Carleer, R. Colins, F. Fally, M. F. Merienne, A. Jenouvrier, and B. Coquart (1997), Measurements of NO_2 absorption cross-sections at 42000 cm^{-1} to 10000 cm^{-1} (238–1000 nm) at 220 K and 298 K, *J. Quant. Spectrosc. Radiat. Transfer*, *59*, 171–184.

Vandaele, A. C., et al. (2005), An intercomparison campaign of ground-based UV-visible measurements of NO_2, BrO, and OClO slant columns: Methods of analysis and results for NO_2, *J. Geophys. Res.*, *110*, D08305, doi:10.1029/2004JD005423.

Volkamer, R. A., U. Platt, and K. Wirtz (2001), Primary and secondary glyoxal formation from aromatics: Experimental evidence for the bicycloalkyl − Radical pathway from benzene, toluene, and p-xylene, *J. Phys. Chem.*, *105*(33), 7865–7874, doi:10.1021/jp010152w.

Volkamer, R. A., L. T. Molina, M. J. Molina, T. Shirley, and W. H. Brune (2005a), DOAS measurement of glyoxal as an indicator for fast VOC chemistry in urban air, *Geophys. Res. Lett.*, *32*, L08806, doi:10.1029/2005GL022616.

Volkamer, R. A., P. Spietz, J. P. Burrows, and U. Platt (2005b), High-resolution absorption cross-section of glyoxal in the UV-vis and IR spectral ranges, *J. Photochem. Photobiol. A Chem.*, *172*(1), 35–46.

Volkamer, R., F. San Martini, L. T. Molina, D. Salcedo, J. L. Jimenez, M. J. Molina, and F. S. Martini (2007), A missing sink for gas-phase glyoxal in Mexico City: Formation of secondary organic aerosol, *Geophys. Res. Lett.*, *34*, L19807, doi:10.1029/2007GL030752.

Vountas, M., A. Richter, F. Wittrock, and J. P. Burrows (2003), Inelastic scattering in ocean water and its impact on trace gas retrievals from satellite data, *Atmos. Chem. Phys.*, *3*, 1365–1375.

Vrekoussis, M., F. Wittrock, A. Richter, and J. P. Burrows (2010), GOME-2 observations of oxygenated VOCs: What can we learn from the ratio glyoxal to formaldehyde on a global scale?, *Atmos. Chem. Phys.*, *10*, 10,145–10,160, doi:10.5194/acp-10-10145-2010.

Wagner, T. (2004), MAX-DOAS O 4 measurements: A new technique to derive information on atmospheric aerosols—Principles and information content, *J. Geophys. Res.*, *109*, D22205, doi:10.1029/2004JD004904. [Available at http://www.agu.org/pubs/crossref/2004/2004JD004904.shtml, Accessed 21 June 2011.]

Wittrock, F. (2006), The retrieval of oxygenated volatile organic compounds by remote sensing techniques, Univ. of Bremen.

Wittrock, F., H. Oetjen, A. Richter, S. Fietkau, T. Medeke, A. Rozanov, and J. P. Burrows (2004), MAX-DOAS measurements of atmospheric trace gases in Ny-Alesund—Radiative transfer studies and their application, *Atmos. Chem. Phys.*, *4*, 955–966.

Wittrock, F., A. Richter, H. Oetjen, J. P. Burrows, M. Kanakidou, S. Myriokefalitakis, R. A. Volkamer, S. Beirle, and U. Platt (2006), Simultaneous global observations of glyoxal and formaldehyde from space, *Geophys. Res. Lett.*, *33*, L16804, doi:10.1029/2006GL026310.